

## Frequency dependence of the local ac magnetic response in type-II superconductors

R. Prozorov, A. Shaulov,\* Y. Wolfus, and Y. Yeshurun  
*Department of Physics, Bar-Ilan University, 52900 Ramat-Gan, Israel*  
 (Received 24 February 1995)

The *local* ac magnetic response in type-II superconductors is analyzed on the basis of the critical state model, taking into account magnetic relaxation effects. The results show that the frequency must be introduced as an independent parameter to the model, in addition to the shielding current which itself is a function of frequency. Using a simplified model for the relaxation law, the calculated frequency dependence of the third harmonic response compares well with experimental data obtained in a Y-Ba-Cu-O crystal. Application of this analysis to ac measurements of magnetic relaxation in the short time limit is discussed.

### INTRODUCTION

Magnetic measurements using alternating fields have been widely employed in the study of superconductors.<sup>1-6</sup> One of the main advantages offered by this “ac” technique is the ability to change the effective time window in the experiment, simply by changing the frequency of the driving field. This feature has found useful applications in the study of magnetic relaxation effects and flux dynamics.<sup>7-10</sup> A comprehensive analysis of the ac response was first given by Bean,<sup>11</sup> based on his critical state model. In a recent study, Shatz, Shaulov, and Yeshurun<sup>12</sup> have shown that in the framework of the Bean model and regardless of the field dependence of the critical current, the global ac response is determined by a *single parameter* which is the ratio between the full penetration field and the amplitude of the applied alternating field. This implies that data of the ac response as a function of any experimental variable (e.g., temperature, dc field, amplitude of the ac field, etc.), can be reduced to a universal curve that describes the response as a function of a single parameter. As a particular result, the peak heights of the harmonic susceptibilities should be universal constants for all type-II superconductors. This conclusion is borne out in many experiments<sup>12</sup> in which the variable-parameter is either the dc field or the amplitude of the ac field. However, recent results<sup>10</sup> on Y-Ba-Cu-O (YBCO) crystals, depicted in Fig. 1, exhibit a strong dependence of the peak height and the peak position on frequency. The figure shows a significant reduction in the third harmonic response,  $V_3$ , as the frequency increases in a relatively narrow range (0.17–17.7 kHz). In addition, the peak of  $V_3$  versus temperature becomes narrower and its position shifts toward higher temperatures as the frequency increases. Similar results were reported by van der Beek *et al.*<sup>13</sup> who measured the third harmonic transmittivity  $T_3$  versus temperature in Bi-Sr-Ca-Cu-O crystals in the frequency range 0.9–2403 Hz. Their data show a monotonous decrease in the peak height of  $T_3$  with frequency. It is thus apparent that the frequency cannot be incorporated in the single-parameter description.

Effects of frequency on the ac response were previously analyzed by Gilchrist and Konczykowski<sup>14</sup> modeling the superconductor as one or two inductively coupled loops. This

analysis was particularly aimed toward understanding the results of “screening” experiments in which two coils are placed on either side of a planar sheet or film to measure the transmittivity of the sample. Our approach in this paper is to analyze the *local* ac response as measured by a miniature Hall probe placed on the surface of the sample. Our calculation is based on the Bean model, taking into account magnetic relaxation effects. Analyzing the local response rather than the global response explains the role of frequency in a most elementary way. We show that magnetic relaxation influences the ac response not only through the frequency dependence of the shielding current density  $j_s$ , but also introduces the frequency as an additional parameter to the model. The single parameter approach<sup>12,15</sup> becomes valid in the limit of high frequencies where magnetic relaxation effects can be neglected.

### ANALYSIS

To illustrate our method of calculation we refer to Fig. 2 which describes the evolution of the magnetic induction profiles in a sample during one period of an applied ac field,

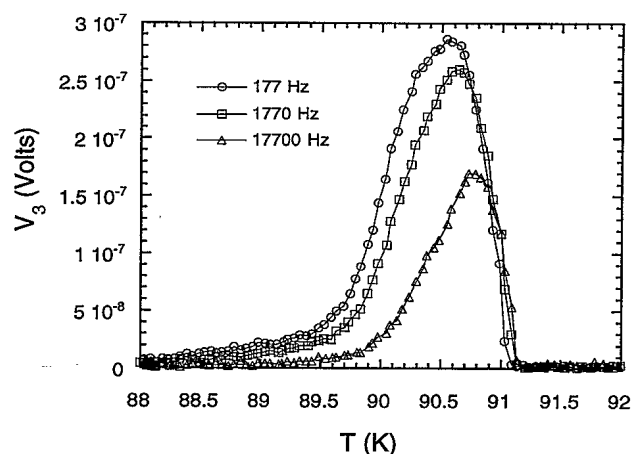


FIG. 1. Temperature dependence of the third harmonic response  $V_3(T)$  in Y-Ba-Cu-O crystal for the indicated frequencies [after Wolfus *et al.* (Ref. 10)]. Note the pronounced frequency dependence of the peak height and the width.

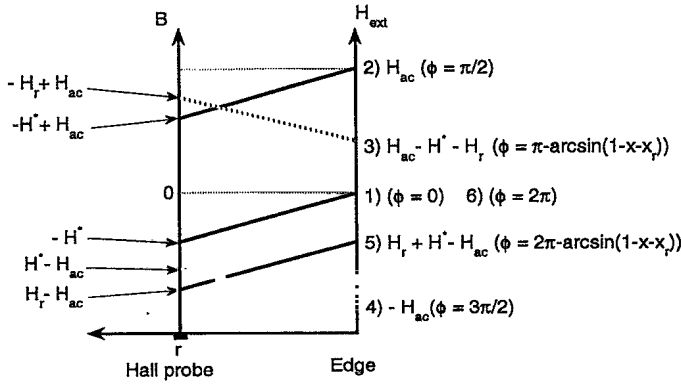


FIG. 2. Schematic description of magnetic induction profiles during one cycle of the applied ac field. A miniature Hall probe is located at a distance  $r$  from the edge of the sample ( $r=0$ ). The profiles 1–6 refer to different times during the ac period; see text.

superimposed on a dc field  $H_{dc}$ . We assume that a miniature Hall probe is located at a distance  $r$  from the nearest edge of the sample located at  $r=0$ . Note that the magnetic induction profiles are depicted in Fig. 2 as straight lines only for simplicity. We start from the moment at which the applied ac field is zero (point 1 in Fig. 2). As the ac field  $h_{ac}=H_{ac}\sin(\varphi)$  increases, the magnetic induction at the Hall probe location follows the field up to the point where the applied ac field reaches its maximum value at  $\varphi=\pi/2$  (point 2 in Fig. 2). At this moment the magnetic induction at the Hall-probe location is  $B_0=H_{ac}-H^*$ , where  $H^*$  is the “local penetration field,” defined as the smallest value of the ac field for which oscillations of  $B$  reach the Hall probe.<sup>15</sup> When  $h_{ac}$  decreases from point 2, the magnetic induction at the edge of the sample is affected immediately; however, it takes time for the external field to reach a value required to affect the induction at the Hall probe location. During this time period,  $B_0$  is not affected by the changes in the external ac field, however it increases due to magnetic relaxation effects. At the end of this time period (point 3 in Fig. 2) the external change in the magnetic field reaches the Hall probe at a phase value  $\varphi_r$  corresponding to time  $t_r$ . In order to calculate  $\varphi_r$ , let us assume that between stages 2 and 3,  $B_0$  has relaxed from  $H_{ac}-H^*$  to  $H_{ac}-H_r$ . Then, according to Fig. 2,

$$H_{ac}-H^*-H_r=H_{ac}\sin(\varphi_r) \quad (1)$$

or

$$1-x-x_r=\sin\left(\frac{\pi}{2}+\omega t_r\right)=\cos(\omega t_r), \quad (2)$$

where  $x=H^*/H_{ac}$  and  $x_r=H_r/H_{ac}$ .

Once the ac field has reached the Hall probe, we assume that the local induction follows the changes in the external field until the latter changes its sign (point 4 in Fig. 2). Thus, in order to calculate the wave form of the local induction during half a cycle, one needs to calculate  $t_r$  from Eq. (2), and the time dependence of the local induction during the time period  $\{0, t_r\}$ . Using similar arguments one can calculate the wave form of the local induction during the second half of the cycle (from point 4 to 5 and back to point 1). From Eq. (2) it is clear that  $t_r$  is a function of  $x$ ,  $x_r$ , and the frequency  $\omega$ . The parameter  $x_r$  is determined by the relaxation law and  $x$ . Accordingly, the ac response depends on  $x$ ,  $\omega$ , and the relaxation law. This is the main result of our analysis. It shows that magnetic relaxation affects directly the ac response by introducing the frequency as an additional parameter to the model. The frequency affects the response also indirectly through the parameter  $x$  which depends on the shielding current which itself is a function of frequency.

In order to calculate  $t_r$  explicitly and the behavior of the local induction in the time period  $\{0, t_r\}$ , one must engage some analytical form for the relaxation law. At high enough frequencies (small  $t_r$ ) one may assume a linear dependence of  $H_r$  upon time:  $H_r=H^*(1-t/t_0)$ , where  $t_0(T, H_{dc})>t_r$  is a characteristic time which depends on temperature and the applied dc field. Such a simplified time dependence serves as an illustration, since it allows us to obtain a relatively simple analytical expression for the local induction. Inserting  $x_r=x(1-t_r/t_0)$  in Eq. (2) results in

$$x+x\left(1-\frac{t_r}{t_0}\right)\approx\frac{(\omega t_r)^2}{2} \quad (3)$$

from which  $t_r$  can be calculated:

$$\omega t_r=\frac{x}{\omega t_0}\left(\sqrt{1+\frac{4\omega^2 t_0^2}{x}}-1\right). \quad (4)$$

For  $x_r$  and  $\varphi_r$  one obtains

TABLE I. Magnetic induction  $B_z(\varphi)$  at the Hall probe location during one cycle of the ac field.

$h_{ac}$	$B(\varphi)$	$\varphi$
$0 \rightarrow H_{ac}$	$H_{ac}\sin(\varphi)-H^*$	$0 \rightarrow \pi/2$
$H_{ac} \rightarrow H_{ac}-H^*-H_r$	$H_{ac}-H^*\left(1-\frac{\varphi-\pi/2}{\omega t_0}\right)$	$\pi/2 \rightarrow \pi-\arcsin(1-x-x_r)$
$H_{ac}-H^*-H_r \rightarrow -H_{ac}$	$H_{ac}\sin(\varphi)+H^*$	$\pi-\arcsin(1-x-x_r) \rightarrow 3\pi/2$
$-H_{ac} \rightarrow -H_{ac}-H^*+H_r$	$-H_{ac}+H^*\left(1-\frac{\varphi-3\pi/2}{\omega t_0}\right)$	$3\pi/2 \rightarrow 2\pi-\arcsin(1-x-x_r)$
$-H_{ac}+H^*+H_r \rightarrow 0$	$H_{ac}\sin(\varphi)-H^*$	$2\pi-\arcsin(1-x-x_r) \rightarrow 2\pi$

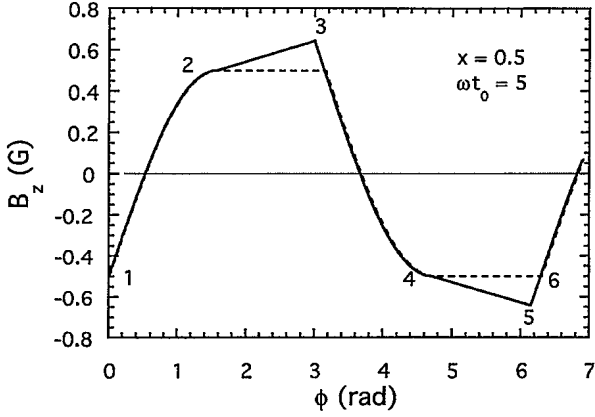


FIG. 3. Wave forms of the magnetic induction during one cycle, for  $x = H^*/H_{ac} = 0.5$ , with  $(\omega t_0 = 5)$  and without relaxation (solid and dotted lines, respectively). Numbers correspond to the stages in Fig. 2.

$$x_r = x \left( 1 - \frac{t_r}{t_0} \right) \approx x \left( 1 - \frac{x \left( \sqrt{1 + \frac{4\omega^2 t_0^2}{x}} - 1 \right)}{\omega^2 t_0^2} \right), \quad (5)$$

$$\varphi_r \approx \pi - \arcsin \left( 1 - 2x + \frac{x^2 \left( \sqrt{1 + \frac{4\omega^2 t_0^2}{x}} - 1 \right)}{\omega^2 t_0^2} \right). \quad (6)$$

Table I gives the functional form of the local magnetic induction  $B_z$  during one cycle, and Fig. 3 illustrates the wave form of  $B_z$  as calculated from this table for  $x = 1/2$ . For comparison, the wave form of  $B_z$ , ignoring magnetic relaxation effects, is also illustrated (dotted curve in Fig. 3). It is seen that due to relaxation the "cutoff" in the second stage is not constant but varies with time (linearly in our approximation). At this stage the time is related to the phase through  $\omega t = \varphi - \pi/2$ .

Once the wave form of  $B_z$  is known, the real part  $\chi'_n$ , imaginary part  $\chi''_n$ , and magnitude  $A_n = \sqrt{(\chi'_n)^2 + (\chi''_n)^2}$  of the local harmonic susceptibilities can be calculated:

$$\begin{cases} \chi'_n \\ \chi''_n \end{cases} = \frac{1}{H_{ac}} \int_0^{2\pi} B(\varphi) \begin{cases} \sin(n\varphi) \\ \cos(n\varphi) \end{cases} d\varphi \quad (7)$$

(note that in the normal state our definition gives  $\chi'_1 = \pi$ ). The global harmonic susceptibilities of the entire sample can be calculated by integration:

$$X_n = \frac{\delta}{\pi} \int_0^k \chi_n(x) dx, \quad (8)$$

where  $\delta = H_{ac}/H_p$  is the parameter of the global response defined in Ref. 12, (inversely) analogous to our local parameter  $x$ , and  $H_p$  is the field of full penetration up to the center of a sample. The upper integration limit

$$k = \begin{cases} 1/\delta & \text{if } \delta \geq 1 \\ 1 & \text{if } \delta \leq 1 \end{cases}. \quad (9)$$

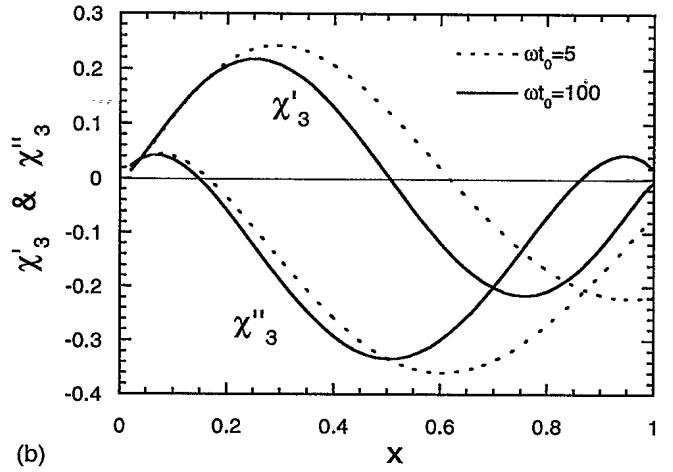
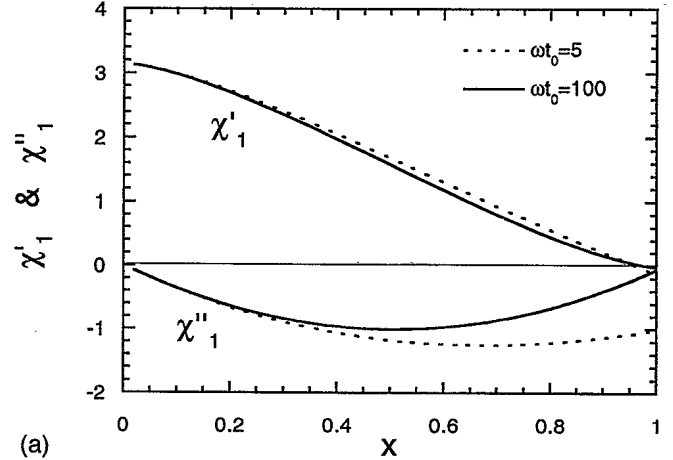


FIG. 4. Harmonic susceptibilities  $\chi_n$  for  $n=1$  (upper frame) and  $n=3$  (lower frame), as a function of  $x = H^*/H_{ac}$ , calculated from Eq. (7) and Table I; see text.

Analytical expressions for  $\chi_n$  can be obtained from Table I using Eq. (7). Because of the complexity of these expressions we prefer to present the results in a graphical form. We use these expressions to show, in Figs. 4(a) and 4(b), the harmonic susceptibilities  $\chi_n$  ( $n=1,3$ ) as a function of  $x$  for two values of frequency corresponding to  $\omega t_0 = 5$  and 100. It is seen that the frequency has strong effects on both the peak height as well as the width of the curves. In order to compare our theoretical results with experiments, we plot in Fig. 5 the absolute value of the third harmonic  $A_3$  as a function of temperature. Here we have assumed exponential temperature dependence of shielding current<sup>12</sup> and  $t_0 \sim (1 - T/T_c)^2$ . A comparison between Figs. 1 and 5 shows that the main experimental observations are satisfactorily described by our analysis; i.e., the peak height of  $V_3$  decreases and the location of the peak is shifted towards higher temperature as the frequency increases. Obviously, a quantitative comparison in the whole temperature range between the experimental results and our model can be made knowing the explicit form of the temperature dependence of the shielding current and the exact relaxation law in the material.

As a particular application of the above analysis, we outline below a method to obtain the short-time relaxation law  $j_s(\omega)$ . For example, one can measure the third harmonic

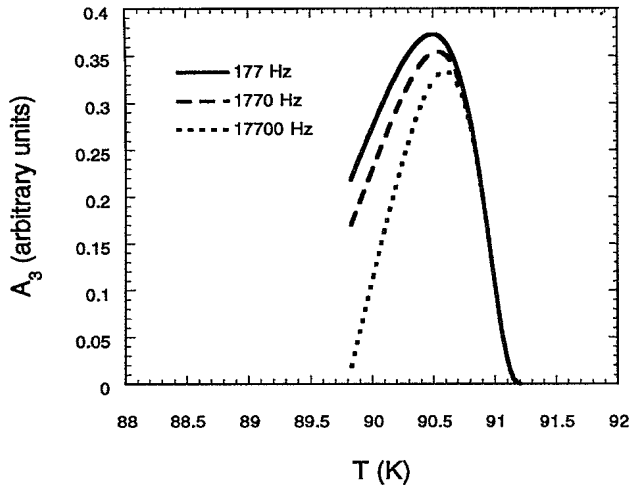


FIG. 5. Third harmonic signal  $A_3 = \sqrt{(\chi_3')^2 + (\chi_3'')^2}$  as a function of temperature, calculated from Eq. (7) and Table I for various frequencies; see text. The qualitative similarity to the experimental data of Fig. 1 is apparent.

susceptibility  $\chi_3$  as a function of  $H_{ac}$  at various frequencies  $\omega$ , at a constant dc magnetic field, and temperature. The peak height  $A_3^p(\omega)$  of each curve is a function of the parameter  $\omega t_0$  alone. Thus by fitting  $A_3^p(\omega)$  to the theoretical prediction one can determine  $t_0$ . The location  $H_{ac}^p$  at which the peak in  $\chi_3$  occurs is a function of both  $x$  and  $\omega t_0$ . Using the previously determined value of  $t_0$  and the experimental values for the location of the peaks, one can determine the  $x$  values,  $x^p(\omega)$ , corresponding to the peaks. Hence one can calculate  $H^*(\omega) = x^p(\omega)H_{ac}^p(\omega)$ , which relates to the shielding current through a numerical factor  $\gamma$ , determined by the sample geometry.<sup>15</sup> We note that our simplification of a linear relaxation does not contradict a situation where the latter

procedure yields a nonlinear  $j_s(\omega)$ ; while the above procedure yields the effective value of  $H^*(\omega)$  in a wide frequency range, the time  $t_r$  is short and one can make a linear approximation for any relaxation law.

## CONCLUSIONS

We have analyzed the local ac magnetic response on the basis of the critical state model, taking into account magnetic relaxation effects. Our analysis shows that these effects introduce the frequency as an additional parameter to the model. The exact dependence of the ac response upon frequency depends on the relaxation law of the shielding current. Using a simplified linear relaxation law, we have demonstrated the salient features exhibited by the third harmonic response  $V_3(T)$  in YBCO crystals; namely the peak height of  $V_3(T)$  decreases and its location is shifted towards higher temperature as the frequency increases. Using our analysis, one may determine the relaxation of the shielding current from ac measurements, e.g., by measuring the frequency dependence of the peak height of the third harmonic response. This method is particularly useful in the short time limit (millisecond range and below) where conventional magnetic techniques for relaxation measurements do not work. A detailed description of this technique and analysis of experimental data will be given elsewhere.

## ACKNOWLEDGMENTS

This work has been supported by the DG XII, Commission of the European Communities, the Israeli Ministry of Science and the Arts (MOSA), and by the Israel Science Foundation administered by the Israeli Academy of Science and Humanities (Project No. 817/94-1). One of us (A.S.) acknowledges support from the France-Israel cooperation program administered by MOSA and by the French Ministry of Research and Technology.

\*On leave from Philips Laboratories, Briarcliff-Manor, New York 10510.

<sup>1</sup>See, e.g., *Magnetic Susceptibility of Superconductors and other Spin Systems*, edited by R. A. Hein, T. L. Francavilla, and D. H. Liebenberg (Plenum, New York, 1991).

<sup>2</sup>A. Shaulov and D. Dorman, *Appl. Phys. Lett.* **53**, 2680 (1988).

<sup>3</sup>L. Ji, R. H. Sohn, G. C. Spalding, C. J. Lobb, and M. Tinkham, *Phys. Rev. B* **40**, 10 936 (1989).

<sup>4</sup>T. Ishida and R. B. Goldfarb, *Phys. Rev. B* **41**, 8937 (1990).

<sup>5</sup>D. G. Xenikos and T. R. Lemberger, *Phys. Rev. B* **41**, 869 (1990).

<sup>6</sup>A. Shaulov Y. Yeshurun, S. Shatz, R. Hareuveni, Y. Wolfus, and S. Reich, *Phys. Rev. B* **43**, 3760 (1991).

<sup>7</sup>P. L. Gammel, M. F. Schneemeyer, and D. J. Bishop, *Phys. Rev. Lett.* **66**, 953 (1991).

<sup>8</sup>P. Seng, R. Gross, U. Baier, M. Rupp, D. Koelle, R. P. Huebener,

P. Schmitt, G. Saemann-Ischenko, and L. Schultz, *Physica C* **192**, 403 (1992).

<sup>9</sup>J. Deak, M. McElfresh, J. R. Clem, Z. Hao, M. Konczykowski, R. Muenchausen, S. Foltyn, and R. Dye, *Phys. Rev. B* **47**, 8377 (1993).

<sup>10</sup>Y. Wolfus, Y. Abulafia, L. Klein, V. A. Larkin, A. Shaulov, Y. Yeshurun, M. Konczykowski, and M. Feigel'man, *Physica C* **224**, 213 (1994).

<sup>11</sup>C. P. Bean, *Rev. Mod. Phys.* **36**, 31 (1964).

<sup>12</sup>S. Shatz, A. Shaulov, and Y. Yeshurun, *Phys. Rev. B* **48**, 13 871 (1993).

<sup>13</sup>C. J. van der Beek, M. Konczykowski, V. M. Vinokur, G. W. Crabtree, T. W. Li, and P. H. Kes (unpublished).

<sup>14</sup>J. Gilchrist and M. Konczykowski, *Physica C* **212**, 43 (1993).

<sup>15</sup>R. Prozorov, A. Shaulov Y. Wolfus, and Y. Yeshurun, *J. Appl. Phys.* **76**, 7621 (1994).